NASA Technical Memorandum 100186

Hydrogen Oxidation Mechanism With Applications to (1) the Chaperon Efficiency of Carbon Dioxide and (2) Vitiated Air Testing

Theodore A. Brabbs, Erwin A. Lezberg, David A. Bittker, and Thomas F. Robertson
Lewis Research Center
Cleveland, Ohio

September 1987

NASA

HYDROGEN OXIDATION MECHANISM WITH APPLICATIONS TO (1) THE CHAPERON EFFICIENCY OF CARBON DIOXIDE AND (2) VITIATED AIR TESTING

Theodore A. Brabbs, Erwin A. Lezberg,
David A. Bittker, and Thomas F. Robertson
National Aeronautics and Space Administration
Lewis Research Center
Cleveland, Ohio 44135

E-3672

SUMMARY

Ignition delay times for the hydrogen/oxygen/carbon dioxide/argon system were obtained behind reflected shock waves. A detailed kinetic mechanism modeled our experimental hydrogen/oxygen data, Skinner and Ringrose's high-pressure data, and Slack and Grillo's hydrogen/air data. A carbon dioxide chaperon efficiency of 7.0 ± 0.2 was determined. The reaction pathway $HO_2 \rightarrow H_2O_2 \rightarrow OH \rightarrow H$ was required to model the high-pressure data. It is suggested that some of the lowest temperature data points (1.0 and 0.5 atm) for Slack and Grillo's hydrogen/air experiments are in error. It was found that the technique of simplifying a detailed kinetic mechanism for a limited range of experimental data may render the model useless for other test conditions.

Ignition delay times for two National Aerospace Plane engine test facilities with different propellant combinations, (1) monomethyl hydrazine/nitrogen tetroxide/oxygen/nitrogen and (2) propane/oxygen/air were modeled. Preliminary analyses indicate that the oxides of nitrogen strongly affect the ignition delay time.

INTRODUCTION

When hydrogen is admitted to a stream of high-temperature air, initiation reactions produce small quantities of atoms and free radicals. These atoms and free radicals then grow in an exponential fashion via a branched-chain kinetic scheme. When sufficient concentrations of atoms and free radicals are attained, there is an exponential rise in the temperature and pressure. The time interval between heating the mixture and the exponential pressure and temperature rise is called the ignition delay time.

At the low static temperatures and moderate pressures used to study supersonic combustion of hydrogen with vitiated air, the progress of the reaction is inhibited by the three-body reaction $H + O_2 + M \rightleftharpoons HO_2 + M$. The amount of inhibition is a function of the pressure, the temperature, and the chaperon efficiency of the third-body molecule (M). For example, as little as 10 percent water vapor (chaperon efficiency, 21.3) in stoichiometric hydrogen/air (at 1 atm and 960 K) increases the ignition delay time from 0.31 to 14.2 msec. Experimentally determined values for the chaperon efficiency of water range from 18.4 to 71. Since vitiated air may contain as much as 30 percent water vapor, there is a definite need for a more accurate determination of its third-body efficiency.

Recently, Stein, Yetter, and Dryer (ref. 1), using a flow tube reactor, reported values for the chaperon efficiency of water vapor and carbon dioxide.

The value they reported for carbon dioxide was much larger than those in the present literature and should be confirmed before one accepts their water value.

The objective of this research was to determine the third-body efficiency of carbon dioxide in a shock tube and to compare it with the value reported by Stein et al. Therefore, we obtained ignition delay times behind reflected shock waves for two gas mixtures. The first mixture, containing 4 percent hydrogen, 2 percent oxygen, and 94 percent argon, was used to develop a kinetic mechanism to model the ignition delay times. The second mixture, containing the same hydrogen and oxygen concentrations, had 10 percent carbon dioxide added to it. The data for this mixture was used to derive the third-body efficiency of carbon dioxide with the aid of the kinetic mechanism developed to model the first mixture.

RESULTS AND DISCUSSION

Ignition Delay Times

The apparatus and experimental details have been described in a previous publication (ref.2). The ignition delay time was measured by monitoring the pressure history behind the reflected shock wave. The quartz pressure transducer located 7 mm from the reflecting surface was used for this measurement. A nylon holder was designed to completely isolate the pressure transducer from the metal walls of the shock tube. This holder produced a very quiet pressure history and allowed us to measure the time when the pressure first started to rise (fig. 1).

The ignition delay time measured in these experiments was defined as the time interval between shock reflection and the initial rise in the ignition pressure. The pressure change at the time of the initial rise is estimated to be about 2 percent. A typical pressure history is shown in figure 1. A gas composition of 4 percent hydrogen, 2 percent oxygen, and 94 percent argon was selected because it produced delay times greater than 100 μsec in the desired temperature range. This is important, since previous work (ref.3) suggests that even at a location 7 mm from the reflecting surface, a small but significant error results when delay times are less than 100 μsec. Ignition delay time measurements for temperatures over 1300 K could not be used since they were quite difficult to measure because the amplitude of the experimental ignition pressure steadily decreased as the reaction temperature increased. The lower temperature limit was imposed by the maximum available test time behind reflected shock waves. The ignition delay times measured for the two gas mixtures are shown in figures 2 and 3.

Schott and Kinsey (ref. 4) showed that the ignition delay time for all of their data could be scaled as delay time x oxygen concentration. Since all of our data were obtained from gas mixtures containing 2 percent oxygen, delay time x pressure was plotted against reciprocal temperature. The dashed line of figure 2 represents Schott and Kinsey's incident-shock-wave data calculated for our gas mixture by their correlation equation:

$$\log_{10}([O_2]\tau) = -10.647 + 3966/T$$

The agreement is very good for shock tube data. Their incident-shock-wave data are about 20 percent lower than the present reflected shock-wave-data. This behavior is exactly what one would expect when incident-shock-wave data have not been corrected for boundary layer effects. Belles and Brabbs (ref. 5) showed that the residence time would be 4 to 16 percent longer when corrections for the boundary layer are applied. The solid line shows the predictions of our kinetic model.

Kinetic Mechanism

Ignition delay times were calculated with the chemical kinetic computer code of Radakrishnan and Bittker (ref. 6) and the kinetic mechanism in table I. The hydrogen oxidation mechanism consists of 20 reversible reactions among 8 reacting species (Table I shows reactions (1) to (20).) Reverse rates were calculated via the equilibrium constant and the forward rates. All rate constants are listed as expressed in the references and any variations in the rates are shown in the Adjustment factor column. The computed ignition delay time was defined as the time at which the pressure increases 2 percent: this time corresponds to our best estimate of the experimental pressure rise at the measured ignition delay time.

The kinetic model was fitted to the high-temperature data by varying the rates of reactions (2), (3), and (7):

$$H + O_2 \leftrightharpoons OH + O \quad (2)$$
$$O + H_2 \leftrightharpoons OH + H \quad (3)$$
$$H_2 + O_2 \leftrightharpoons OH + OH \quad (7)$$

The rate for reaction (2) was increased 20 percent, which is well within the experimental error of the data. This increase brought the rate to within 10 percent of the value recommended by Baulch et al. (ref.7) and into agreement with the value recommended by Roth and Just (ref. 8). Jachimowski and Houghton (ref. 9) studied the initiation reaction (7) and determined a value of 1.7×10^{13} exp (-48150/RT) for the rate constant. According to them, the rate constant was good to within a factor of 3. Thus, an adjustment factor of 2 for this reaction is well within their error. At the low-temperature end of the data, the model was fitted by small adjustments in reactions (4) and (12):

$$H + O_2 + M \leftrightharpoons HO_2 + M \quad (4)$$
$$H + HO_2 \leftrightharpoons OH + OH \quad (12)$$

Reaction (12) is the primary path by which HO_2 molecules are consumed in the low-pressure region. This rate constant was increased by 20 percent.

Once a fit to the data was established, the kinetic mechanism was simplified by removing reactions which were found to be unimportant when fitting the present data. At this time, we encountered one of the pitfalls associated with mechanism simplification: The new mechanism modeled the present data very well, but it completely missed Skinner and Ringrose's high-pressure data (ref. 10), and in some cases ignition did not occur. This problem resulted because the reaction pathway $HO_2 \rightarrow H_2O_2 \rightarrow OH \rightarrow H$ was omitted in the reduced mechanism. This pathway is very important in the high-pressure region where the rate of production of HO_2 via reaction (4) is much faster than the rate

of branching via reaction (2). This illustrates how reducing a detailed kinetic mechanism to only the important reactions for a limited range of experimental data can render the mechanism useless for other test conditions.

The set of rate constants used for reactions (13) to (19) were taken from Dixon-Lewis and Williams (ref. 11) rather than Lloyd (ref. 12) because of the difference in the recommended value for reaction (17):

$$HO_2 + HO_2 \rightleftharpoons H_2O_2 + O_2 \qquad (17)$$

The activation energy Lloyd assigned to the reaction was shown by Troe et al. (refs. 13 and 14) to be incorrect. Since some of the other reactions depend on the rate of reaction (17), the rate constants assigned to reactions (13) to (19) were taken from reference 11. The best fit to the high-pressure data (fig. 4) required a 20-percent increase in the rate constant for reaction (19):

$$H_2O_2 + M \rightleftharpoons OH + OH + M \qquad (19)$$

Comparison of Kinetic Model with Hydrogen/Air Data

One may wonder whether a kinetic mechanism developed from shock tube measurements of gas mixtures highly diluted with argon can be used for modeling practical gas systems. The stoichiometric hydrogen/air ignition-delay-time data of Slack and Grillo (ref. 15) allow one to test the appropriateness of such an approach to kinetic modeling.

Slack and Grillo measured ignition delay times for stoichiometric hydrogen/air over the temperature range 1450 to 850 K and at four pressures (2.0, 1.0, 0.5, and 0.27 atm). The ignition delay times predicted by our proposed model are compared with Slack and Grillo's data in figure 5. Ignition delay times were calculated for two commonly used third-body efficiencies of nitrogen and oxygen (1.5 and 1.3). The best fit to the data was obtained for an efficiency of 1.3, which is the value recommended by Baulch et al. (ref. 7). The model predictions are in good agreement with the data for the three highest pressures and for temperatures above 950 K. The disagreement between the model predictions and the 0.27 atm data is somewhat surprising since at this pressure ignition depends only on reactions (2), (3), and (7), whose rates are all well known. It is believed that this data may be affected by either slow vibrational relaxation of nitrogen or the maximum test time behind very low pressure shock waves. The lack of agreement between the model predictions and the data below 950 K is the same behavior that Hitch et al. (ref. 16) reported in their study of three hydrogen/air kinetic mechanisms. In this temperature region, all three models predicted longer delay times than Slack and Grillo measured. Two observations became apparent. First, the 0.5 and 1.0 atm data do not show the large increase in delay time with a small decrease in the temperature that are shown by Slack and Grillo's 2.0-atm and our 1.1-atm data. Second, the longest delay times measured are about 1 msec. A possible explanation for this behavior is that these measured delay times are affected by the maximum available test time.

The maximum test time behind a reflected shock wave is the time interval between shock reflection and the arrival of the reflected disturbance produced by the interaction between the reflected shock wave and the contact surface.

This reflected disturbance can be either a shock wave or a rarefaction wave. Figure 1 shows that the reflected disturbance for our experimental setup is a shock wave. This shock wave can easily cause a reacting mixture to ignite. The maximum test time calculated for our test apparatus was 3.1 msec, which compares well with the average experimental value of 3.3 msec. For the apparatus used by Slack and Grillo (ref. 15), we calculated a test time of 1.2 msec for a 15-ft test section, and of 1.0 msec for a 12-ft test section. The agreement between the calculated maximum test times and the delay times measured for these low-temperature experiments, suggests that the data are a measure of the maximum test time and not the ignition delay time for hydrogen/air.

Carbon Dioxide Chaperon Efficiency

The chaperon efficiency for carbon dioxide was determined by modeling the ignition delay times obtained for the hydrogen/oxygen mixture containing 10 percent carbon dioxide. The calculation with the detailed mechanism is a straight-forward procedure because the third-body efficiency of carbon dioxide is the only adjustable parameter. For completeness, the reactions of carbon dioxide with H atoms and OH radicals must be added to the hydrogen/oxygen mechanism:

$$CO + OH \rightleftharpoons CO_2 + H \qquad (21)$$

$$CO + HO_2 \rightleftharpoons CO_2 + OH \qquad (22)$$

Note that the actual rate constants used are for the reverse of these two reactions because they are better known. Model predictions for a chaperon efficiency of 1.0 for carbon dioxide showed that the carbon dioxide molecule was not inert.

The delay times calculated were found to be about 2 percent longer than those calculated for the hydrogen/oxygen mixture. This difference was produced by the slight inhibiting affect of reaction (21), which competes with reactions (2) and (4) for H atoms. The best fit to the hydrogen/oxygen/carbon dioxide data is for a chaperon efficiency of 7.0, which is shown in figure 7. The carbon dioxide chaperon efficiency of 7.0 ± 0.2 relative to argon is in good agreement with the value of 7.3 found by Lewis and Von Elbe (ref. 17), and is slightly larger than the value of 5.0 recommended by Baulch et al. (ref. 7). However, it is much smaller than the value of 14 relative to nitrogen, or 21 relative to argon suggested by Stein et al. (ref. 1). Model predictions for this value of the chaperon efficiency are shown in figure 6.

Vitiated Air Effects on Scramjet Ignition

The hydrogen/oxygen/argon kinetic mechanism in table I was extended to include reactions for the hydrogen/oxygen/nitrogen system (table II). This kinetic mechanism was used to model ignition of hydrogen/vitiated air for two NASP engine test facilities (ETF's). ETF-1 produced vitiated air via the propellant combination monomethyl hydrazine/nitrogen tetroxide/oxygen/nitrogen and ETF-2 produced vitiated air via the propellant combination propane/oxygen/air. Table III compares the hydrogen/vitiated air mixtures at the start of the ignition calculation for the two test facilities. The table

shows that ETF-1 contains more water but less carbon dioxide than ETF-2 and that both contain equal and significant amounts of NO_x.

The propellant combination stoichiometry for each test facility was adjusted to simulate the Mach 8 stagnation temperature and pressure (2611 K and 190.6 atm) for flight at an altitude of about 90,000 ft. For each test facility, the mole fraction in the propellants was adjusted so that the oxygen mole fraction in the combustion products was the same as for air. The combustion products were expanded in equilibrium to a slightly supersonic Mach number and then expanded kinetically to a Mach number of 6.5. This simulated the design Mach numbers for the ETF nozzles. However, a simple conical expansion, rather than a contoured design, was assumed for the facility nozzle.

Since the one-dimensional kinetics program could not simulate the compression process through an engine inlet, the product composition was assumed to be frozen at the Mach 6.5 condition, and at the static pressure, temperature, and Mach numbers specified at the combustor entrance station. These conditions were taken from scramjet cycle calculations. A mixture temperature was then calculated for the addition of a stoichiometric amount of hydrogen at a temperature of 667 K.

Kinetic calculations of the combustion process were performed for both vitiated airs and a standard dry air composition for two combustor entrance conditions resulting from different inlet contraction ratios. Calculations were performed for each of these inlet conditions for both constant-area and divergent-area combustor geometries.

RESULTS

The ignition process is shown in figure 7 as pressure versus distance in centimeters for a constant-area combustor geometry at a mixture temperature of about 1000 K. Ignition was deemed to occur when there was a near vertical rise in the pressure. Comparisons of ignition for vitiated air from the two test facilities and for dry air at the same temperature are shown in this figure. Differences in ignition are relatively minor (approximately 5 percent) for the two ETF's, but these ignition distances are considerably shorter than that calculated for air. Calculations for a divergent-area (area ratio, 1.8) combustor geometry are shown in figure 7. Again the difference in ignition distances is minor (approximately 7 percent), but in this case air did not ignite in the 81-cm combustor length. Table IV compares the calculated distance for the ETF's and air at two inlet conditions and for two combustor geometries.

DISCUSSION

Ignition of hydrogen in the temperature range of 950 to 1050 K and at pressures above 1 atm are controlled by the competition for hydrogen atoms by the branched-chain reaction

$$H + O_2 \leftrightharpoons OH+O \qquad (2)$$

and the termination reaction

$$H + O_2 + M \leftrightharpoons HO_2 + M \qquad (4)$$

The HO_2 radical is a fairly unreactive product. The rate of reaction (4) is critically dependent on the pressure and the chaperon efficiency of the third-body molecule (M). If M is water or carbon dioxide, the efficiencies are considerably higher than for nitrogen, hydrogen, and oxygen and one would assume that ignition delays for vitiated air products and hydrogen would be longer than for air and hydrogen. This is not the case: ignition distances calculated for the two ETF's were much shorter than that calculated for air (fig. 6). A comparison of the ignition distance for ETF-1 with that of ETF-2 shows the small, but measurable, inhibiting effect of water.

In any heating process, when the temperatures are high enough, thermal NO_x is produced (NO and NO_2). The sum of the mole fractions of these species remains relatively constant during expansion through a facility nozzle. Thus, the reaction mechanism in the scramjet combustor becomes much more complicated. The reaction

$$NO + HO_2 \leftrightharpoons NO_2 + OH \qquad (25)$$

followed by

$$H_2 + OH \leftrightharpoons H_2O + H \qquad (1)$$

prevents the build up of HO_2 and regenerates the hydrogen atoms necessary for ignition. NO is regenerated by reaction (28),

$$NO_2 + H \leftrightharpoons NO + OH \qquad (28)$$

almost as fast as it is consumed by reaction (25). For the cases examined in this paper, although the NO_x entering the scramjet test engine has a mole fraction of only about 0.9 percent, it has a dominant effect on the ignition distance. It offsets the inhibiting effect of the large amounts of water and carbon dioxide in the vitiated products.

During flight through the atmosphere, however, it is unlikely that significant amounts of nitric oxide can be formed in the inlet compression process except at very high Mach numbers or possibly in the boundary layer because the formation reactions are relatively slow. Hence, the hydrogen atom removal through formation of HO_2 becomes dominant even with the lower chaperon efficiency of the diatomic molecules.

It has been shown elsewhere that even smaller concentrations of oxides of nitrogen can substantially shorten ignition delays for hydrogen/air mixtures. Thus, the addition of NO_x, perhaps in the form of nitrogen tetroxide, may provide an effective ignition source for hydrogen at marginal conditions.

REFERENCES

1. Stein, Y.; Yetter, R.; and Dryer, F.: Flow Reactor Studies of the Reaction $H + O_2 + M \rightarrow HO_2 + M$. Proceedings, 1986 Fall Meeting Eastern Section Combustion Institute, Dec. 1986, Paper 28.

2. Brabbs, T.A.; and Robertson, T.F.: The Carbon Dioxide Chaperon Efficiency for the Reaction $H + O_2 + M \rightarrow HO_2 + M$ From Ignition Delay Times Behind Reflected Shock Waves. NASA TM-100125, 1987.

3. Brabbs, T.A.; and Robertson, T.F.; Methane Oxidation Behind Reflected Shock Waves - Ignition Delay Times Measured by Pressure and Flame Band Emission. NASA TM-87268, 1986.

4. Schott, G.L.; and Kinsey, J.L.: Kinetic Studies of Hydroxyl Radicals in Shock Waves. II. Induction Times in the Hydrogen-Oxygen Reaction. J. Chem. Phys., vol. 29, no. 5, Nov. 1958, pp. 1177-1182.

5. Belles, F.E.; and Brabbs, T.A.: Experimental Verification of Effects of Turbulent Boundary Layers on Chemical-Kinetic Measurements in a Shock Tube. Thirteenth Symposium (International) on Combustion, The Combustion Institute, Pittsburgh, 1970, pp. 165-175.

6. Radakrishnan, K.; and Bittker, D.A.: GCKP86 - An Efficient Code for General Chemical Kinetics and Sensitivity Analysis Computations. Proceedings, 1986 Fall Meeting Eastern Section Combustion Institute, Dec. 1986, Paper 46.

7. Baulch, D.L., et al.: Evaluated Kinetic Data for High Temperature Reactions. Vol. 1, Homogeneous Gas Phase Reactions of the H_2-O_2 System. CRC Press, 1972.

8. Roth, P.; and Just, T.H.: Kinetics of the High Temperature, Low Concentration CH_4 Oxidation Verified by H and O Atom Measurements. Twentieth Symposium (International) on Combustion, The Combustion Institute, Pittsburgh, 1984, pp. 807-818.

9. Jachimowski, C.J.; and Houghton, W.M.: Shock-Tube Study of the Initiation Process in the Hydrogen-Oxygen Reaction. Combust. Flame, vol. 17, 1971, pp. 25-30.

10. Skinner, G.B.; and Ringrose, G.H.: Ignition Delays of a Hydrogen-Oxygen-Argon Mixture at Relatively Low Temperatures. J. Chem. Phys., vol. 41, no. 6, Mar. 15, 1965, pp. 2190-2192.

11. Dixon-Lewis, G.; and Williams D.J.: The Oxidation of Hydrogen and Carbon Monoxide. Comprehensive Chemical Kinetics, vol. 17, Gas-Phase Combustion, C.H. Bamford and C.F.H. Tipper, eds., Elsevier Scientific, 1977, Chapter 1, pp. 1-248.

12. Lloyd, A.C.: Evaluated and Estimated Kinetic Data for Phase Reactions of the Hydroperoxyl Radical. Int. J. Chem. Kinet., vol. 6, no. 2, Mar. 1974, pp. 169-228.

13. Troe, J.: Ultraviolet Spectrum and Reactions of the HO_2 Radical in the Thermal Decomposition of Hydrogen Peroxide. Ber. Bunsenges Phys. Chem., vol. 73, no. 10, 1969, pp. 946-952.

14. Baulch, D.L.; Drysdale, D.D.; and Horne, D.G.: An Assessment of Rate Data for High-Temperature Systems. Fourteenth Symposium (International) on Combustion, The Combustion Institute, Pittsburgh, 1973, pp. 107-118.

15. Slack, M.W.; and Grillo, A.: Investigation of Hydrogen-Air Ignition Sensitized by Nitric Oxide and by Nitrogen Dioxide. NASA CR-2896, 1977.

16. Hitch, B.D., et al.: Studies of Selected Hydrogen-Air Kinetic Mechanisms for Use in Supersonic Combustor Modeling. Presented at the Second ASME-JSME Thermal Engineering Joint Conference, Honolulu, HI, Mar. 1986.

17. Von Elbe, G.; and Lewis, B.: The Reaction Between Hydrogen and Oxygen: The Upper Explosion Limit and Reaction in its Vicinity. J. Chem. Phys., vol. 9, no. 2, Feb. 1941, pp. 194-195.

18. Von Elbe, G.; and Lewis, B.: Mechanism of the Thermal Reaction Between Hydrogen and Oxygen. J. Chem. Phys., vol. 10, no. 6, June 1942, pp. 366-393.

TABLE I. - HYDROGEN/OXYGEN REACTIONS

Reaction number	Reaction	Rate coefficient[a]			
		Adjustment factor	A	n	E
1	$OH + H_2 \rightleftharpoons H_2O + H$	----	2.1×10^{13}	0	5 100
2	$H + O_2 \rightleftharpoons OH + O$	1.2	1.38×10^{14}	0	16 400
3	$O + H_2 \rightleftharpoons OH + H$	1.1	2.96×10^{13}	0	9 800
4	$H + O_2 + M \rightleftharpoons HO_2 + M$	.95	2.1×10^{18}	-1.0	----
5	$H_2 + M \rightleftharpoons H + H + M$	----	2.2×10^{14}	0	96 000
6	$O_2 + M \rightleftharpoons O + O + M$	----	1.8×10^{18}	-1.0	118 020
7	$H_2 + O_2 \rightleftharpoons OH + OH$	2.0	1.7×10^{13}	0	48 150
8	$H_2O + M \rightleftharpoons H + OH + M$	----	2.2×10^{16}	↓	105 140
9	$O + H_2O \rightleftharpoons OH + OH$	----	6.8×10^{13}	↓	18 365
10	$H + HO_2 \rightleftharpoons H_2 + O_2$	----	1.4×10^{13}	↓	----
11	$O + HO_2 \rightleftharpoons OH + O_2$	----	5.0×10^{13}	↓	1 000
12	$H + HO_2 \rightleftharpoons OH + OH$	1.2	1.7×10^{14}	↓	1 070
13	$OH + HO_2 \rightleftharpoons H_2O + O_2$	----	8.0×10^{12}	↓	2 980
14	$H + HO_2 \rightleftharpoons O + H_2O$	----	1.7×10^{13}	↓	1 070
15	$H_2 + HO_2 \rightleftharpoons H_2O_2 + H$	----	6.0×10^{11}	↓	18 500
16	$OH + H_2O_2 \rightleftharpoons H_2O + HO_2$	----	6.1×10^{12}	↓	1 430
17	$HO_2 + HO_2 \rightleftharpoons H_2O_2 + O_2$	----	2.0×10^{12}	↓	----
18	$H + H_2O_2 \rightleftharpoons OH + H_2O$	----	7.8×10^{11}	↓	----
19	$M + H_2O_2 \rightleftharpoons OH + OH$	1.2	1.2×10^{17}	↓	45 510
20	$O + H + M \rightleftharpoons OH + M$	----	7.1×10^{18}	-1.0	----
21	$CO + OH \rightleftharpoons CO_2 + H$	----	4.17×10^{11}	0	1 000
22	$CO + HO_2 \rightleftharpoons CO_2 + OH$	----	5.75×10^{13}	0	22 930

[a] $k = AT^n \exp(-E/RT)$ in units of mol, cm^3, sec, cal.

TABLE II. - HYDROGEN/OXYGEN/NITROGEN REACTIONS

Reaction number	Reaction	Rate coefficient[a]		
		A	n	E
23	$CO + O + M \rightleftharpoons CO_2 + M$	5.9×10^{15}	0	4 100
24	$CO + O_2 \rightleftharpoons CO_2 + O$	2.5×10^{12}		47 690
25	$HO_2 + NO \rightleftharpoons NO_2 + OH$	2.09×10^{12}		-477
26	$O + NO_2 \rightleftharpoons NO + O_2$	1.0×10^{13}		596
27	$NO + O + M \rightleftharpoons NO_2 + M$	5.62×10^{15}		-1 160
28	$NO_2 + H \rightleftharpoons NO + OH$	3.47×10^{14}		1 470
29	$NO + H \rightleftharpoons N + OH$	2.63×10^{14}		50 410
30	$NO + O \rightleftharpoons N + O_2$	3.8×10^{9}	1.0	41 370
31	$O + N_2 \rightleftharpoons NO + N$	1.82×10^{14}	0	76 250
32	$N + NO_2 \rightleftharpoons 2NO$	4.0×10^{12}	0	0
33	$N_2O + M \rightleftharpoons N_2 + O + M$	6.92×10^{23}	-2.5	65 000
34	$O + N_2O \rightleftharpoons N_2 + O_2$	1.0×10^{14}	0	28 020
35	$O + N_2O \rightleftharpoons 2NO$	6.92×10^{13}		26 630
36	$N_2O + H \rightleftharpoons N_2 + OH$	7.59×10^{13}		15 100
37	$N_2O + H_2 \rightleftharpoons HNO_2 + H$	2.4×10^{13}		29 000
38	$OH + NO_2 + M \rightleftharpoons HNO_3 + M$	3.0×10^{15}		-3 800
39	$OH + NO + M \rightleftharpoons HNO_2 + M$	5.6×10^{15}		-1 700
40	$HNO + H \rightleftharpoons H_2 + NO$	5.0×10^{12}		0
41	$H + NO + M \rightleftharpoons HNO + M$	5.4×10^{15}		-600
42	$HNO + OH \rightleftharpoons H_2O + NO$	3.6×10^{13}		0

[a] $k = AT^n \exp(-E/RT)$ in units of mol, cm^3, sec, cal.

TABLE III. - MAJOR SPECIES OTHER THAN OXYGEN, HYDROGEN, AND NITROGEN

Species	Composition of mixture in test facilities, percent		
	ETF-1[a]	ETF-2[b]	ETF-1/ETF-2
CO_2	5.9	9.8	0.60
H_2O	17.7	13.1	1.35
NO	.9	.92	1.0
NO_2	.025	.025	1.0

[a] Propellant used in engine test facility 1 (ETF-1), monomethyl hydrazine/nitrogen tetroxide/oxygen/nitrogen.

[b] Propellant used in ETF-2, propane/oxygen/air.

TABLE IV. - CALCULATED IGNITION DISTANCE FOR TWO ENGINE TEST FACILITIES - ETF-1 AND ETF-2 - AND STANDARD AIR

	Temperature, K	Pressure, atm	Ignition distance, cm	
			Combustor geometry	
			Constant area	Divergent area
ETF-1[a]	960 1002	3.1 2.7	27.2 12.5	no ignition 18.6
ETF-2[b]	957 999	3.1 2.7	26.0 11.9	no ignition 17.4
H_2/air	992 961 961 961	2.7 2.7 2.0 1.0	70 no ignition no ignition 50	no ignition ↓ ↓ ↓

[a]Propellant used in ETF-1, monomethyl hydrazine/ nitrogen tetroxide/oxygen/nitrogen.
[b]Propellant used in ETF-2, propane/oxygen/air.

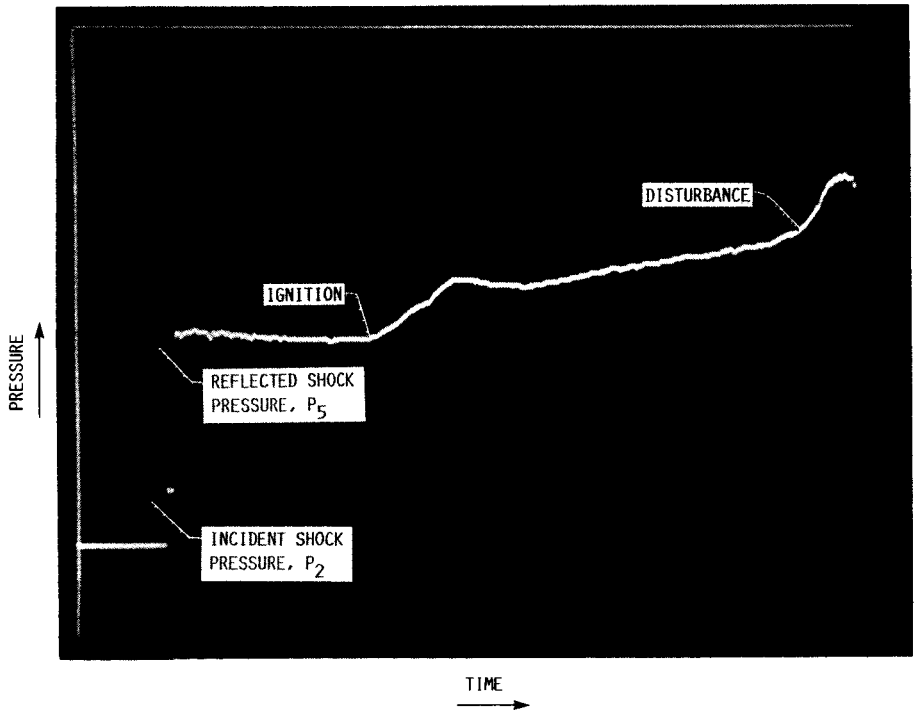

FIGURE 1. - TYPICAL PRESSURE HISTORY 7 mm FROM END OF SHOCK TUBE.

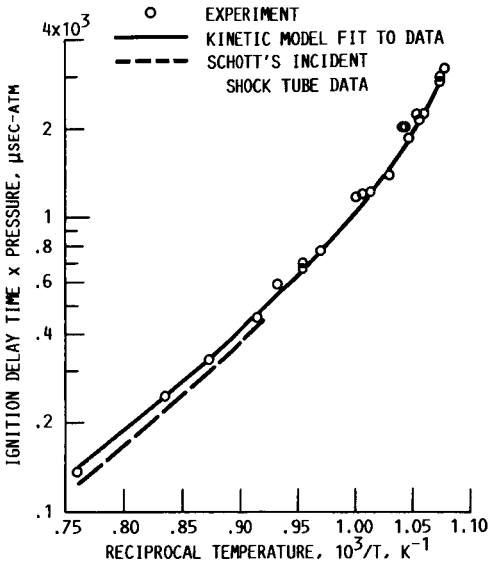

FIGURE 2. - PRODUCT OF IGNITION DELAY TIME AND PRESSURE VERSUS RECIPROCAL TEMPERATURE FOR 4 PERCENT HYDROGEN/2 PERCENT OXYGEN/94 PERCENT ARGON MIXTURE. DASHED LINE CALCULATED FROM SCHOTT'S CORRELATION EQUATION, $\log_{10}[O_2]\tau = 10.647 + 3966/T$ (REF. 4).

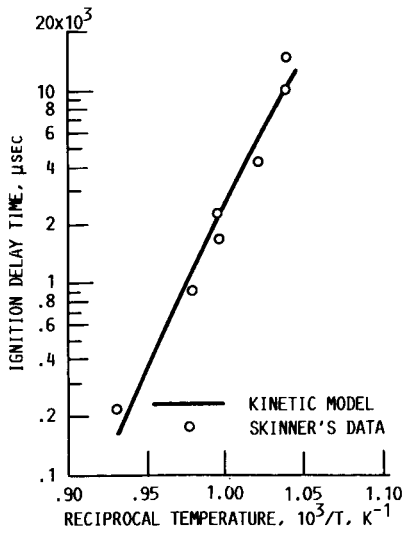

FIGURE 4. - IGNITION DELAY TIMES MEASURED BY SKINNER AT A PRESSURE OF 5.0 ATM FOR 8 PERCENT HYDROGEN/2 PERCENT OXYGEN/90 PERCENT ARGON MIXTURE (REF. 10).

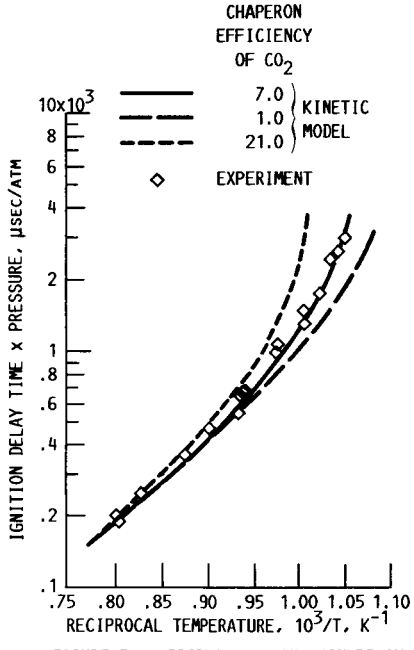

FIGURE 3. - PRODUCT OF IGNITION DELAY TIME AND PRESSURE VERSUS RECIPROCAL TEMPERATURE FOR 4 PERCENT HYDROGEN/2 PERCENT OXYGEN/10 PERCENT CARBON DIOXIDE/84 PERCENT ARGON MIXTURE. BEST FIT TO THE DATA BY THE KINETIC MECHANISM WAS FOR A CARBON DIOXIDE CHAPERON EFFICIENCY OF 7.0.

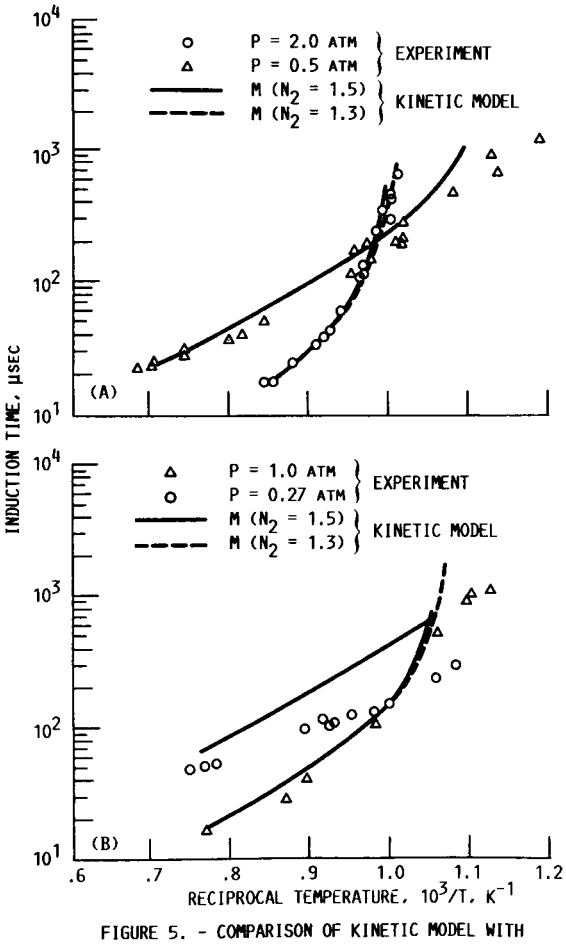

FIGURE 5. - COMPARISON OF KINETIC MODEL WITH STOICHIOMETRIC HYDROGEN/AIR IGNITION DELAY TIMES MEASURED BY SLACK FOR FOUR PRESSURES (REF. 15).

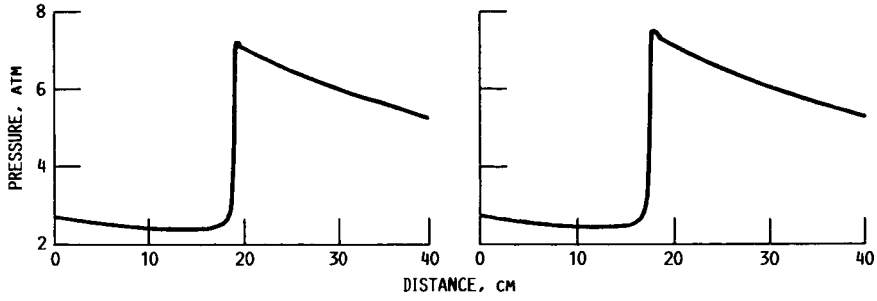

(A) ETF-1. (B) ETF-2.

FIGURE 6. - CALCULATED PRESSURE PROFILE FOR COMBUSTION OF HYDROGEN IN A DIVERGENT-AREA COMBUSTOR (AREA RATIO, 1.8) AS FUNCTION OF COMBUSTOR LENGTH FOR TWO ENGINE TEST FACILITIES - ETF-1 AND ETF-2.

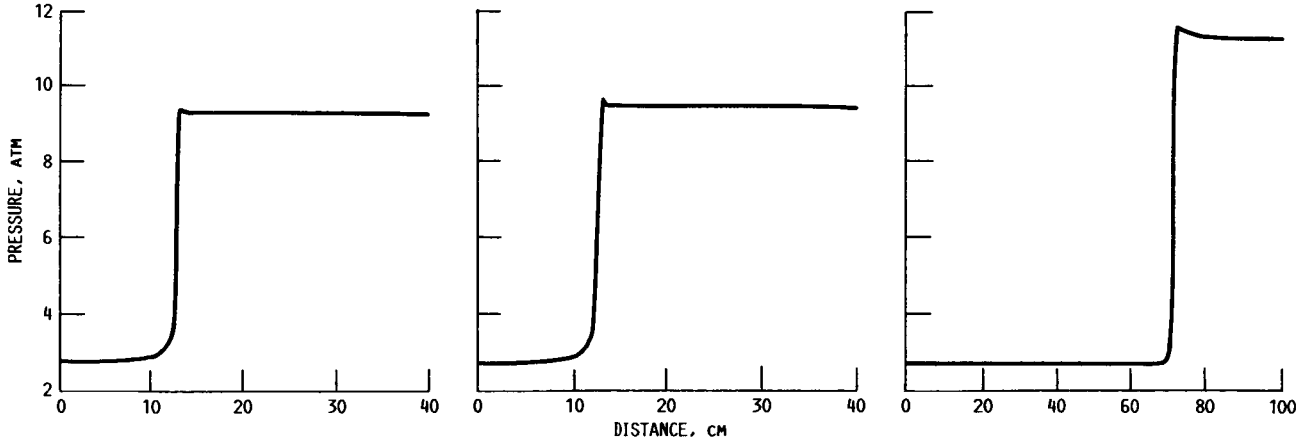

(A) ETF-1. (B) ETF-2. (C) STANDARD AIR.

FIGURE 7. - CALCULATED PRESSURE PROFILE FOR COMBUSTION OF HYDROGEN IN A CONSTANT-AREA COMBUSTOR AS FUNCTION OF COMBUSTOR LENGTH FOR TWO ENGINE TEST FACILITIES - ETF-1 AND ETF-2 - AND STANDARD AIR.

NASA
National Aeronautics and Space Administration

Report Documentation Page

1. Report No.	2. Government Accession No.	3. Recipient's Catalog No.
NASA TM-100186		

4. Title and Subtitle

Hydrogen Oxidation Mechanism With Applications to (1) The Chaperon Efficiency of Carbon Dioxide and (2) Vitiated Air Testing

5. Report Date

September 1987

6. Performing Organization Code

7. Author(s)

Theodore A. Brabbs, Erwin A. Lezberg, David A. Bittker, and Thomas F. Robertson

8. Performing Organization Report No.

E-3672

10. Work Unit No.

505-62-21

9. Performing Organization Name and Address

National Aeronautics and Space Administration
Lewis Research Center
Cleveland, Ohio 44135-3191

11. Contract or Grant No.

13. Type of Report and Period Covered

Technical Memorandum

12. Sponsoring Agency Name and Address

National Aeronautics and Space Administration
Washington, D.C. 20546-0001

14. Sponsoring Agency Code

15. Supplementary Notes

16. Abstract

Ignition delay times for the hydrogen/oxygen/carbon dioxide/argon system were obtained behind reflected shock waves. A detailed kinetic mechanism modeled our experimental hydrogen/oxygen data, Skinner and Ringrose's high-pressure data, and Slack and Grillo's hydrogen/air data. A carbon dioxide chaperon efficiency of 7.0 ± 0.2 was determined. The reaction pathway $HO_2 \rightarrow H_2O_2 \rightarrow OH \rightarrow H$ was required to model the high-pressure data. It is suggested that some of the lowest temperature data points (1.0 and 0.5 atm) for Slack and Grillo's hydrogen/air experiments are in error. It was found that the technique of simplifying a detailed kinetic mechanism for a limited range of experimental data may render the model useless for other test conditions.

17. Key Words (Suggested by Author(s))	18. Distribution Statement
Hydrogen/oxygen kinetics Shock waves Ignition delay times Hydrogen/air modeling	Unclassified - Unlimited Subject Category 25

19. Security Classif. (of this report)	20. Security Classif. (of this page)	21. No of pages	22. Price*
Unclassified	Unclassified	14	A02

NASA FORM 1626 OCT 86

*For sale by the National Technical Information Service, Springfield, Virginia 22161